Contribution of the crystalline lens gradient refractive index to the accommodation amplitude in non-human primates: In vitro studies

Bianca M. Maceo
Ophthalmic Biophysics Center, Bascom Palmer Eye Institute & Biomedical Optics and Laser Laboratory, Department of Biomedical Engineering, University of Miami, Miami, FL, USA

Fabrice Manns
Ophthalmic Biophysics Center, Bascom Palmer Eye Institute & Biomedical Optics and Laser Laboratory, Department of Biomedical Engineering, University of Miami, Miami, FL, USA

David Borja
Ophthalmic Biophysics Center, Bascom Palmer Eye Institute & Biomedical Optics and Laser Laboratory, Department of Biomedical Engineering, University of Miami, Miami, FL, USA

Derek Nankivil
Ophthalmic Biophysics Center, Bascom Palmer Eye Institute, University of Miami Miller School of Medicine, Miami, FL, USA

Stephen Uhlhorn
Ophthalmic Biophysics Center, Bascom Palmer Eye Institute, University of Miami Miller School of Medicine, Miami, FL, USA

Esdras Arrieta
Ophthalmic Biophysics Center, Bascom Palmer Eye Institute, University of Miami Miller School of Medicine, Miami, FL, USA

Arthur Ho
Brien Holden Vision Institute, Sydney, Australia, Vision Cooperative Research Centre, Sydney, Australia, & School of Optometry and Vision Science, University of New South Wales, Sydney, NSW, Australia

Robert C. Augusteyn
Vision Cooperative Research Centre, Sydney, Australia, & School of Optometry and Vision Science, University of New South Wales, Sydney, NSW, Australia

Jean-Marie Parel
Ophthalmic Biophysics Center, Bascom Palmer Eye Institute & Biomedical Optics and Laser Laboratory, Department of Biomedical Engineering, University of Miami, Miami, FL, USA, & Vision Cooperative Research Centre, Sydney, Australia

The purpose of this study was to determine the contribution of the gradient refractive index to the change in lens power in hamadryas baboon and cynomolgus monkey lenses during simulated accommodation in a lens stretcher. Thirty-six monkey lenses (1.4–14.1 years) and twenty-five baboon lenses (1.8–28.0 years) were stretched in discrete steps. At each stretching step, the lens back vertex power was measured and the lens cross-section was imaged with optical coherence tomography. The radii of curvature for the lens anterior and posterior surfaces were calculated for each step. The power of each lens surface was determined using refractive indices of 1.365 for the outer cortex and 1.336 for the aqueous. The gradient contribution was calculated by subtracting the power of the surfaces from the measured lens power. In all lenses, the contribution of the surfaces and gradient increased linearly with the amplitude of accommodation. The gradient contributes on average $65 \pm 3\%$ for monkeys and $66 \pm 3\%$ for baboons to the total power change during accommodation. When expressed in percent of the total power change, the relative contribution of the gradient remains constant with accommodation and age in both species. These findings are consistent with Gullstrand's intracapsular theory of accommodation.

Introduction

The crystalline lens has a gradient refractive index due to a non-uniform distribution of protein concentrations within the lens (Augusteyn, 2010; Smith, 2003). This gradient is a unique property of the crystalline lens that significantly contributes to its optical power and aberrations (Atchison & Smith, 2000; Garner & Smith, 1997; Smith, 2003; Tabernero, Berrio, & Artal, 2011). In young lenses, the refractive index gradually increases from the surface of the lens to the center. There is evidence that with increasing age, the refractive index distribution becomes approximately uniform over the central region of the lens, forming a plateau (Augusteyn, Jones, & Pope, 2008; Jones, Atchison, Meder, & Pope, 2005; Moffat, Atchison, & Pope, 2002), and that the size of the plateau increases with age (de Castro et al., 2011; Kasthurirangan, Markwell, Atchison, & Pope, 2008). Studies on isolated lenses suggest that these changes in the refractive index distribution with age decrease both the optical power of the lens and the contribution of the gradient to the lens power (Borja et al., 2008; Borja, Manns et al., 2010; Glasser & Campbell, 1999; Jones et al., 2005). The contribution of the gradient refractive index to the lens power is generally quantified in terms of an "equivalent index," which is the refractive index of a homogeneous lens with the same shape and power as the crystalline lens with gradient index. *In vivo* and *in vitro* studies have shown that the equivalent index decreases with age. (Borja et al., 2008; Borja, Manns et al., 2010; Dubbelman & Van der Heijde, 2001). This finding is consistent with the observation that the contribution of the gradient index to lens power decreases with age.

In addition to age-related changes, alterations in the refractive index profile must also occur during accommodation since the lens changes shape with accommodation. *In vivo* studies using MRI found that the central and peripheral refractive indices do not change significantly with accommodation but that there is a change in the distribution of the refractive index (Kasthurirangan et al., 2008). According to Gullstrand's intracapsular theory of accommodation, changes in the internal structure of the lens contribute to the accommodation amplitude (Gullstrand, 1962/1909, 1911). In order to account for the contribution of the gradient refractive index, Gullstrand used a higher equivalent refractive index in the lens of his schematic eye in the accommodated state than in the relaxed state. However, more recent studies have shown that the equivalent index of the lens does not change during accommodation (Garner & Smith, 1997; Hermans, Dubbelman, Van der Heijde, & Heethaar, 2008).

In vivo measurements of the gradient's contribution to lens accommodation are challenging because they require accurate measurements of the lens shape and rely on indirect measurements of lens power and/or equivalent refractive index (Garner & Smith, 1997). An *ex vivo* lens stretching system that allows us to reproduce disaccommodation in lenses while measuring the changes in lens shape and power was recently developed (Ehrmann, Ho, & Parel, 2008). The purpose of the present study was to use the lens stretcher equipped with an optical coherence tomography (OCT) system (Uhlhorn, Borja, Manns, & Parel, 2008) to directly quantify the contribution of the gradient during simulated accommodation in non-human primate lenses.

Materials and methods

Donor tissue

We report data on 36 lenses from 34 cynomolgus monkeys (*Macaca fascicularis*, postmortem time [PMT], 17.7 ± 12.7 h; ages, 1.4–14.1 years) and 25 lenses from 19 hamadryas baboons (*Papio hamadryas*, PMT, 21.64 ± 12.8 h; ages, 1.8–28.0 years). All experiments adhered to the Association for Research in Vision and Ophthalmology Statement for the Use of Animals in Ophthalmic and Visual Research. The eyes were obtained from the Division of Veterinary Resources at the University of Miami as part of a tissue-sharing protocol and were used in accordance with Institutional Animal Care and Use Guidelines. The eyes were enucleated immediately after euthanasia, wrapped in gauze, and placed in a closed container. No animals were euthanized for the sole purpose of this study. Upon arrival at the laboratory, all eyes were either directly prepared for stretching experiments or refrigerated at 4 °C (Nankivil et al., 2009).

Tissue preparation

All tissue dissections were performed by an ophthalmic surgeon. The tissue preparation protocol has been described in detail elsewhere (Ehrmann et al., 2008; Manns et al., 2007). In summary, the whole globe is bonded to eight scleral attachments (shoes) to maintain the shape of the globe during dissection and stretching. Once the shoes are bonded to the sclera, the posterior pole, cornea, and iris are surgically removed. Incisions are then made in the sclera between adjacent shoes to produce eight segments for stretching. Special attention is paid to keeping the ciliary body intact. The prepared tissue sample, consisting of the ciliary body, zonular fibers, crystalline lens, and the segmented sclera, is mounted in the *Ex Vivo* Accommodation Simulator (EVAS II). EVAS II is a second-generation lens stretching system that reproduces disaccommodation in lenses by simultaneously stretching the eight scleral segments radially in a step-

wise fashion (0.5 mm/step, up to 2.5 mm; Ehrmann et al., 2008). The tissue is immersed in a small chamber filled with Dulbecco's Modified Eagle Medium (DMEM) throughout the experiment to avoid osmotic swelling.

Measurement of anterior and posterior lens curvature and thickness

For all lenses, one stretching run was performed to quantify the changes in lens shape. At each 0.5-mm increment of stretch, the lens was imaged with a custom-designed time-domain optical coherence tomography system using a superluminescent diode with a central wavelength of 825 nm and a bandwidth of 25 nm. The system has an optical scan depth of 10 mm and an axial resolution of 12 μm in air (9 μm in tissue; Uhlhorn et al., 2008). A telecentric beam delivery system is used to produce a meridional B-scan. The delivery system is mounted on a 3-axis translation stage to allow precise centering of the OCT beam in the transverse direction and adjustment of the focus to maximize the signal strength. The beam is aligned before the first stretching step by visualizing the signal intensity along the central A-line in real time and adjusting the position of the delivery optics until the signal peaks corresponding to the anterior and posterior lens surfaces are within the scan depth and maximized. Images were recorded with 5000 points/A-line, 500 A-lines/B-scan, and a lateral scan length of 10 mm or 12 mm depending on the size of the lens (Uhlhorn et al., 2008).

The OCT images are processed using a semiautomatic edge-detection program developed in MATLAB (MathWorks, Natick, MA) to detect the anterior and posterior lens boundaries. Residual lens tilt is corrected using a procedure that has been described elsewhere (Urs, Ho, Manns, & Parel, 2010). The image is scaled in the axial direction to convert optical distances to geometrical distances using the measured group refractive index of DMEM (n = 1.345 at 825 nm; Borja, Siedlecki et al., 2010) and an estimate of the average group refractive index of the crystalline lens based on the age of the primate. We assume that the age dependence of the group refractive index in primates is similar to that of the human lenses in Uhlhorn et al. (2008). A correction factor was applied to convert human age to equivalent primate age (monkey age = human age/3; Borja, Manns et al., 2010). The distortions on the posterior surface due to refraction at the anterior surface of the lens were corrected using an exact ray trace. The distortion correction technique uses the method from Borja, Siedlecki et al. (2010), assuming a uniform refractive index equal to the average index of the lens. The anterior lens shape and corrected posterior lens surface were then fit over the central 3-mm optical zone with a spherical fit to calculate the radius of curvature for the anterior surface, R_a, and posterior surface, R_p. For all lenses, the axial lens thickness was directly measured from the scaled images (Figure 1).

Measurement of lens power

Following the stretching run to measure lens shape, three additional stretching runs were performed to quantify the changes in lens power for all eyes. The power reported is the average of the three measurements obtained at each step. The optical system uses the OCT light source and beam delivery system. For power measurements, the scanners are programmed to produce a circular ring pattern with a 1.5-mm scan radius that is centered on the anterior lens surface. The location posterior to the lens where the ring converges to a single spot is detected by a camera mounted on an adjustable vertical translation stage below the lens. This location corresponds to the focal point in the image space of the lens. A paraxial optical model that takes into account the distance from the posterior lens surface to the window, the thickness of the window, and the distance from the window to the camera sensor is used to calculate the back vertex power of the lens in diopters (D). To quantify the intrinsic accuracy of the power measurements, the system was calibrated using a set of glass lenses of known optical power. The accuracy of the measurements was ±0.5 D. The error may be slightly higher in crystalline lenses due to their lower optical quality.

When tissue is mounted in the lens stretcher (unstretched state), the tension on the ciliary body and zonules is completely relaxed. The first and second stretching steps place the accommodative structures (zonules and ciliary body) under tension. During this stretching phase, the lens shifts slightly upward. In the subsequent steps, the posterior lens surface continues to move upward due to changes in the posterior lens shape. The slight upward movement of the lens is evident in Figure 1. Any translation of the lens or posterior lens surface that occurs during simulated accommodation is accounted for in the power calculations by measuring the displacement of the posterior surface of the lens. The displacement is added to the distance between the posterior surface of the lens and the window, d_p, obtained from a reference image acquired in the unstretched position (Figure 2).

Calculation of the surface and gradient contribution to lens power

To allow for direct comparison with the back vertex power measured during stretching experiments, we calculated the contribution of the lens surfaces and refractive index gradient to back vertex power. We defined the surface contribution as the back vertex power of a thick spherical lens with radii of curvature and thickness equal to
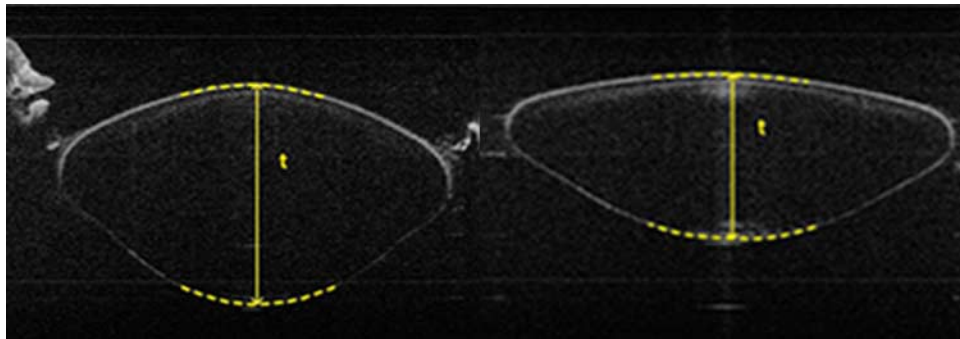
Figure 1. Sample OCT images of a lens during stretching experiments (3.25-year-old baboon). These images are scaled for refractive index but are not corrected for refractive distortion. The dashed lines show the spherical fit of the central 3 mm of the anterior and posterior surfaces. These images are used to measure lens thickness, t. The tissue is shown in the (left) unstretched (accommodated) state and (right) stretched (unaccommodated) state. The radial displacement of the shoes in the stretched state was 2.5 mm. In this particular lens, the dimensions in the unstretched state were: diameter: 8.07 mm; thickness: 4.45 mm; anterior radius: 4.29 mm; posterior radius: 3.49 mm. The dimensions in the stretched state were: diameter: 9.11 mm; thickness: 3.32 mm; anterior radius: 11.44 mm; posterior radius: 5.16 mm. The figure also demonstrates the slight upward movement of the lens. The displacement of the lens posterior surface is measured and taken into account in the calculation of lens power (see text).

those of the crystalline lens and with a uniform refractive index equal to the index of the outer cortex ($n = 1.365$). With this definition, the total contribution of the surfaces, P_s, can be written as

$$P_s = \frac{P_1}{\left(1 - \dfrac{t \cdot P_1}{n}\right)} + P_2, \tag{1}$$

where P_1 is the power of the anterior surface, P_2 is the power of the posterior surface, t is the measured lens thickness, and n is the refractive index of the lens outer cortex (Jenkins & White, 1976). The first term on the right-hand side of Equation 1 is the contribution of the anterior surface power and lens thickness to the back vertex power. The second term is the contribution of the posterior surface power to the back vertex power. The contribution from the thickness term was minimal, corresponding to less than 3% of the anterior surface contribution for all lenses in this study. The change in thickness contributed to less than 0.01 D of the change in power during accommodation for all lenses.
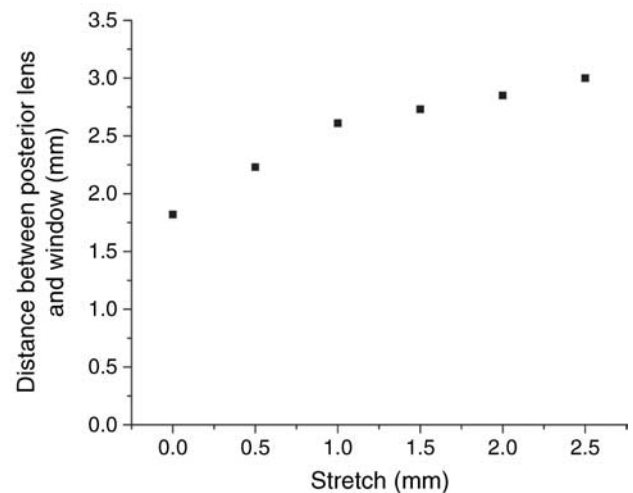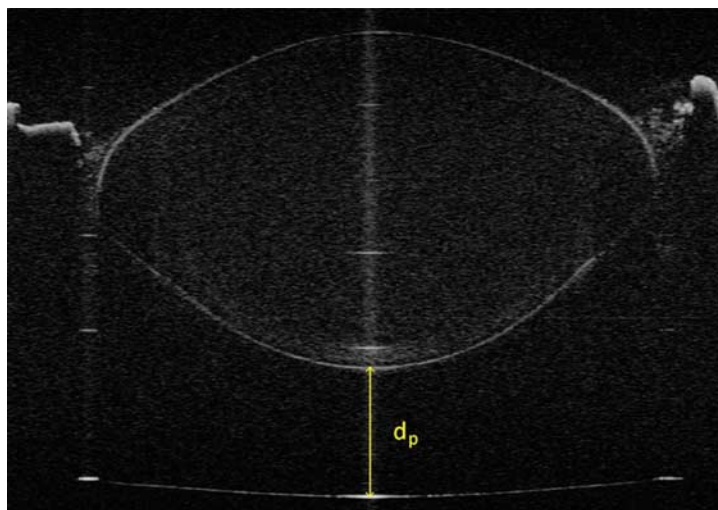

Figure 2. Compensation for the displacement of the lens posterior surface. (Left) Reference image of a 2.3-year-old baboon lens. The image is scaled for refractive index but is not corrected for refractive distortion. This image is used to measure the distance between the posterior surface of the lens and posterior window of the chamber, d_p, in the unstretched position. (Right) Change in the distance between the posterior lens surface and the window during stretching. The displacement of the lens posterior surface for this particular lens is roughly 1.2 mm.
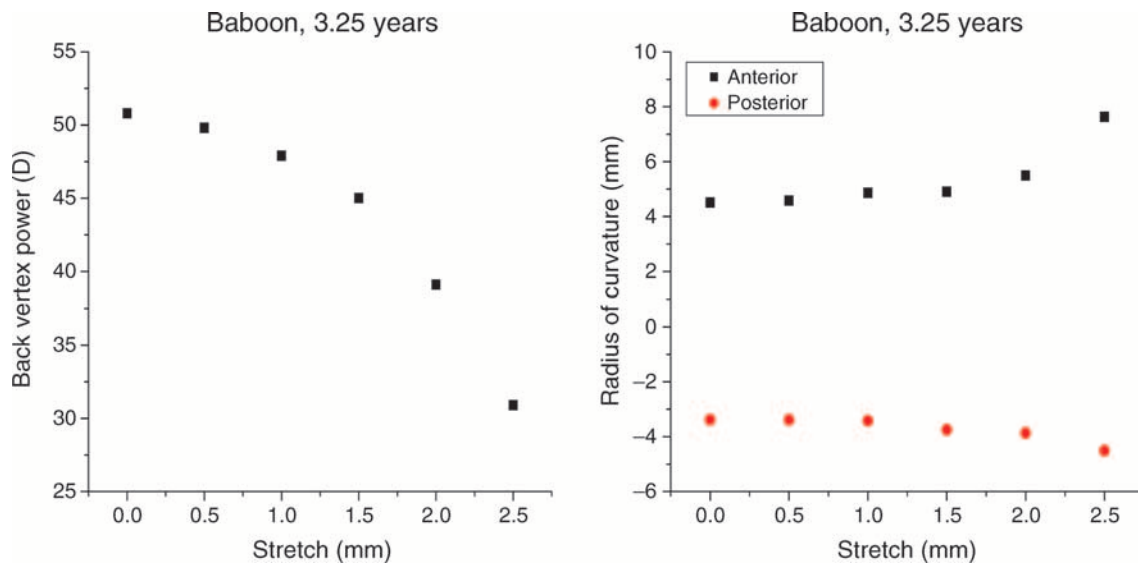
Figure 3. (Left) Typical plot of lens back vertex power (D) with respect to stretch (mm). The power decreases as the lens is stretched from an accommodated state to an unaccommodated state. (Right) Typical plot of anterior and posterior lens radius of curvature (mm) with respect to stretch (mm). The posterior radii of curvature are negative due to the orientation of the lens surface. The anterior and posterior surfaces of the lens flatten as the lens is stretched.

To take into account the effect of spherical aberration, the individual surface powers P_1 and P_2 were calculated for an incident ray height corresponding to the conditions of the power measurement. For the anterior surface, the ray height was 1.5 mm. For the posterior surface, the ray height calculated by the ray tracing algorithm for the distortion correction was used. For each individual surface, the effective focal length at the corresponding ray height was determined using an exact ray trace implemented in MATLAB. The power of the anterior and posterior surfaces, P_1 and P_2, were calculated by converting these focal lengths to dioptric power using a refractive index $n = 1.365$ for the outer cortex and $n_o = 1.336$ for the aqueous.

To calculate the contribution of the gradient within the lens, P_g, the combined calculated power of the anterior and posterior surfaces was subtracted from the measured back vertex power of the lens, P_L:

$$P_g = P_L - P_s. \tag{2}$$

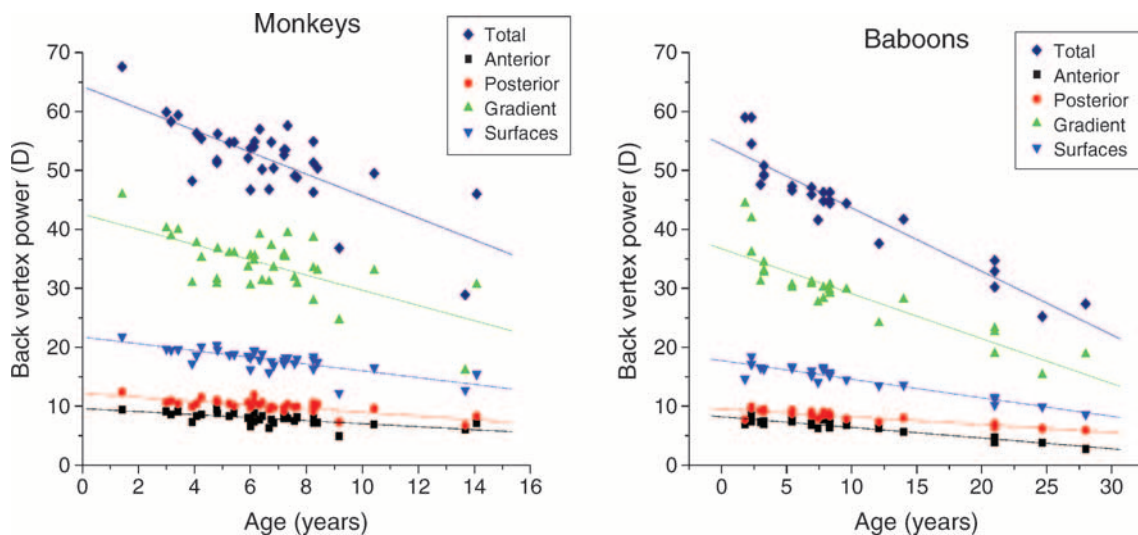Note that the power is measured at 825 nm with a broadband source, while the surface contribution is

Figure 4. Unstretched lens power as a function of age for (left) cynomolgus monkeys and (right) hamadryas baboons. The lens back vertex power and contributions of the lens anterior surface, posterior surface, combined surfaces, and gradient are shown.

Baboon	Age (years)	Unstretched lens back vertex power (D)	Anterior surface unstretched power (D)	Posterior surface unstretched power (D)	Gradient unstretched power (D)	Anterior surface slope (D/D)	Posterior surface slope (D/D)	Gradient slope (D/D)
1 OS	1.80	59.0	6.9	7.7	44.4	0.187	0.122	0.719
2 OD	2.30	59.0	7.4	9.6	41.9	0.154	0.128	0.717
3 OD	2.30	54.5	8.5	9.9	36.1	0.220	0.168	0.611
4 OD	3.00	47.6	7.3	9.2	31.1	0.258	0.225	0.514
5 OD	3.25	49.3	7.1	9.1	33.0	0.189	0.143	0.632
5 OS	3.25	50.8	7.0	9.4	34.4	0.147	0.134	0.718
6 OS	3.67	49.1	7.4	9.1	32.7	0.207	0.155	0.639
7 OD	5.42	47.3	7.4	9.3	30.6	0.218	0.173	0.607
7 OS	5.42	46.6	7.9	8.7	30.1	0.227	0.136	0.639
8 OD	6.92	47.1	7.0	9.0	31.1	0.190	0.094	0.715
8 OS	6.92	45.9	6.8	8.4	30.7	0.223	0.159	0.618
9 OD	7.42	41.6	6.2	7.9	27.6	0.241	0.121	0.639
10 OD	7.83	46.3	7.7	8.5	30.1	0.206	0.130	0.666
10 OS	7.83	44.8	7.7	9.0	28.2	0.134	0.104	0.762
11 OD	8.30	44.9	6.4	8.8	29.7	0.176	0.168	0.651
12 OD	8.33	44.4	7.0	8.3	29.1	0.222	0.138	0.634
12 OS	8.33	46.3	7.1	8.6	30.6	0.185	0.115	0.677
13 OD	9.60	44.4	6.8	7.8	29.8	0.160	0.124	0.696
14 OD	12.10	37.6	6.2	7.3	24.1	0.281	0.123	0.588
15 OS	14.00	41.7	5.6	8.0	28.1	0.159	0.107	0.734
16 OD	21.00	34.7	4.7	6.8	23.2	0.246	0.190	0.572
16 OS	21.00	32.9	3.9	6.4	22.6	0.221	0.106	0.670
17 OD	21.00	30.2	4.3	7.0	18.9	0.207	0.168	0.625
18 OD	24.66	25.2	3.8	6.2	15.3	0.240	0.185	0.590
19 OS	28.00	27.4	2.7	5.9	18.8	NA	NA	NA

Table 1. Hamadryas baboon results. Measured lens back vertex power, anterior surface, posterior surface, and gradient power in the unstretched state and the anterior surface, posterior surface, and gradient contributions to accommodation amplitude (in D/D).

calculated using the phase index at 589 nm. In theory, the measured power should be adjusted to take into account dispersion effects. However, an analysis using the dispersion model of Atchison and Smith (2005) shows that the difference in refractive index between the lens cortex and aqueous is approximately the same whether the phase refractive index at 589 nm ($\Delta n = 0.0290$) or the group refractive at 825 nm ($\Delta n = 0.0296$) is used. The power measurements were therefore not adjusted for dispersion.

Since power measurements are acquired in separate runs from the curvature measurements, variations between runs may introduce errors in the calculated surface contributions. We estimated this error by quantifying the variability between power runs. The relative error was $2.0 \pm 1.2\%$ on average for all lenses in this study. The maximum relative error in the relative surface contribution was 4.0% on average.

Data analysis

The contributions of lens anterior surface, posterior surface, and gradient to total lens power were calculated for all lenses at each stretching step using Equations 1 and 2. The contributions of the surfaces and gradient to the accommodation amplitude were quantified by plotting the individual contributions as a function of total lens power during stretching. The age dependence of the contributions was analyzed.

Results

General behavior

In all lenses, except the 28-year-old (oldest) baboon lens, the anterior and posterior surfaces flattened and total lens power decreased as the lens was stretched, as expected from the Helmholtz theory of accommodation (Figure 3). In the oldest baboon lens, there was no significant change in lens shape during stretching experiments. Therefore, the analysis for this lens is limited to the unstretched state.

Monkey	Age (years)	Unstretched lens back vertex power (D)	Anterior surface unstretched power (D)	Posterior surface unstretched power (D)	Gradient unstretched power (D)	Anterior surface slope (D/D)	Posterior surface slope (D/D)	Gradient slope (D/D)
1 OD	1.42	67.6	9.4	12.4	45.9	0.168	0.168	0.668
2 OD	3.00	59.9	9.1	10.6	40.2	0.192	0.138	0.672
3 OD	3.17	58.3	8.6	10.9	38.8	0.194	0.169	0.636
4 OD	3.42	59.4	9.1	10.4	39.9	0.221	0.126	0.651
5 OD	3.92	48.2	7.3	9.9	30.9	0.215	0.183	0.598
6 OD	4.08	56.3	8.3	10.4	37.7	0.207	0.138	0.652
7 OD	4.25	55.4	8.6	11.5	35.2	0.214	0.182	0.599
8 OD	4.80	51.3	9.7	10.7	30.8	0.225	0.169	0.605
8 OS	4.80	51.7	9.3	11.0	31.5	0.245	0.160	0.596
9 OD	4.83	56.2	8.8	10.7	36.7	0.195	0.143	0.664
10 OS	5.25	54.7	8.3	10.4	36.0	0.212	0.191	0.597
11 OD	5.42	54.8	8.8	10.0	36.0	0.229	0.158	0.613
12 OD	5.92	52.1	8.0	10.6	33.6	0.198	0.178	0.624
13 OS	6.00	53.8	7.8	10.4	35.6	0.216	0.159	0.624
14 OD	6.00	46.7	6.6	9.7	30.5	0.205	0.204	0.592
15 OS	6.13	54.0	7.4	11.9	34.7	0.181	0.197	0.618
16 OD	6.15	54.9	8.8	10.5	35.5	0.217	0.143	0.637
17 OS	6.33	57.0	7.7	10.2	39.1	0.145	0.136	0.716
18 OS	6.42	50.2	8.3	10.6	31.3	0.244	0.220	0.536
19 OD	6.67	46.8	6.3	9.4	31.1	0.217	0.209	0.572
20 OD	6.75	54.8	7.7	9.9	37.2	0.169	0.152	0.681
21 OD	6.83	50.4	7.2	9.7	33.5	0.192	0.177	0.633
22 OS	7.20	53.5	7.9	9.7	35.8	0.215	0.146	0.640
22 OD	7.20	52.6	8.2	9.1	35.4	0.168	0.136	0.697
23 OD	7.25	53.5	8.3	9.9	35.3	0.202	0.150	0.643
24 OS	7.33	57.6	7.9	10.3	39.4	0.184	0.154	0.663
25 OD	7.58	49.1	7.5	9.8	31.8	0.215	0.149	0.636
26 OD	7.67	48.8	8.1	9.9	30.8	0.232	0.174	0.587
27 OD	8.25	46.3	7.9	10.5	27.9	0.235	0.199	0.564
28 OD	8.25	51.3	8.0	9.8	33.4	0.171	0.138	0.698
29 OD	8.25	54.9	7.2	9.1	38.6	0.164	0.141	0.695
30 OD	8.40	50.4	7.2	10.3	33.0	0.201	0.176	0.628
31 OD	9.17	36.8	4.9	7.3	24.6	0.178	0.161	0.657
32 OD	10.42	49.5	6.9	9.6	33.0	0.166	0.168	0.668
33 OD	13.67	28.9	6.0	6.7	16.1	0.351	0.211	0.436
34 OS	14.08	46.0	7.1	8.3	30.6	0.185	0.176	0.639

Table 2. Cynomolgus monkey results. Measured lens back vertex power, anterior surface, posterior surface, and gradient power in the unstretched state and the anterior surface, posterior surface, and gradient contributions to accommodation amplitude (in D/D).

Lens surface and gradient power (D) vs. age (Figure 4)

As reported in previous studies (Borja et al., 2008; Borja, Manns et al., 2010; Jones et al., 2005), the total power of the lens in the unstretched (accommodated) state decreases with age (Figure 4). The power of the gradient decreases with age in both species ($p < 0.001$ for monkeys, $p < 0.001$ for baboons). The power of the anterior and posterior lens surfaces also slightly decreases with age ($p < 0.001$ for monkeys, $p < 0.001$ for baboons). The total power, surface contribution, and gradient contribution of the monkey lenses are higher than those of the baboon lenses. The power data are shown in Tables 1 and 2.

Lens surface and gradient contribution vs. accommodation (in D, Figure 5)

The power of the lens surfaces and gradient decreases linearly as the total lens power decreases during stretching (disaccommodation). The rate of change was quantified by performing a linear regression of the anterior surface, posterior surface, combined surfaces, and gradient contributions. The slope of the linear regression provides
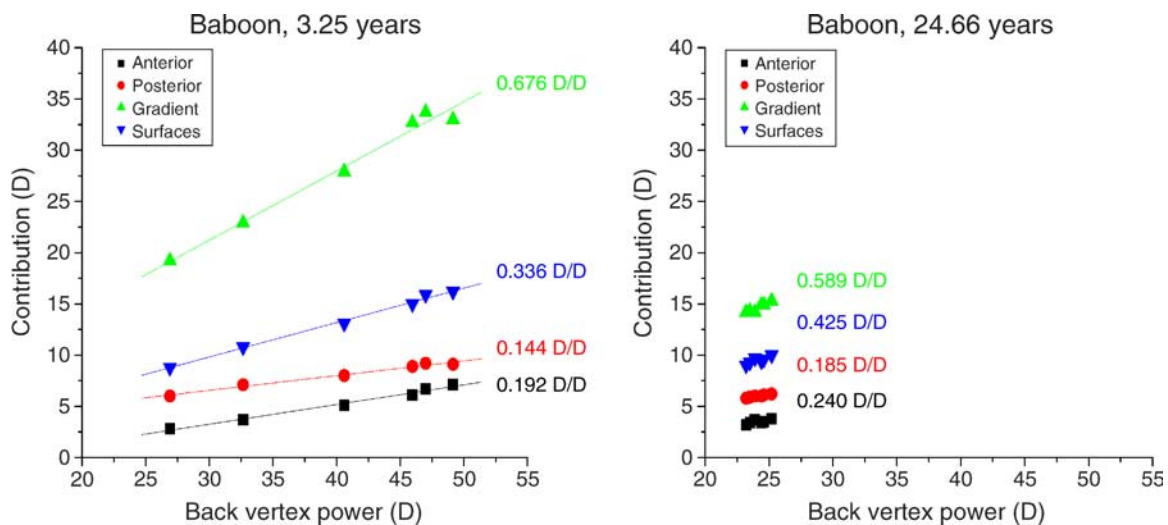
Figure 5. Typical example of the contribution of the lens anterior surface, posterior surface, combined surfaces, and gradient to lens back vertex power during simulated accommodation for (left) a young baboon and (right) an older baboon. For young baboons (age < 14 years), the R^2 values ranged from 0.82 to >0.99 for the anterior surface, 0.84 to >0.99 for the posterior surface, 0.83 to >0.99 for the combined surfaces, and 0.93 to >0.99 for the gradient. For the older baboons (age > 20 years), the R^2 values ranged from 0.81 to 0.93 for the anterior surface, 0.92 to >0.99 for the posterior surface, 0.86 to 0.96 for the combined surfaces, and 0.89 to >0.99 for the gradient. For the monkeys, the R^2 values ranged from 0.98 to >0.99 for the anterior surface, 0.90 to >0.99 for the posterior surface, 0.94 to >0.99 for the combined surfaces, and >0.993 for the gradient.

the contribution of the surfaces or gradient to the accommodation amplitude. The changes in lens power observed during stretching were significantly reduced in the older baboon lenses (Figure 5, right).

Surface and gradient contribution to accommodation amplitude (in D/D, Figure 6)

In all lenses, the contribution of the anterior surface to accommodation amplitude was larger than that of the posterior surface, and the contribution of the gradient was larger than the combined contribution of the surfaces. The contribution of the anterior surface to the accommodation amplitude ranged from 0.14 D/D to 0.35 D/D for the cynomolgus monkeys and 0.13 D/D to 0.28 D/D for the hamadryas baboons. The contribution of the posterior surface to the accommodation amplitude ranged from 0.13 D/D to 0.22 D/D for the cynomolgus monkeys and 0.09 D/D to 0.23 D/D for the hamadryas baboons. The contribution of the gradient remains constant with age in both species ($p = 0.16$ for monkeys, $p = 0.35$ for
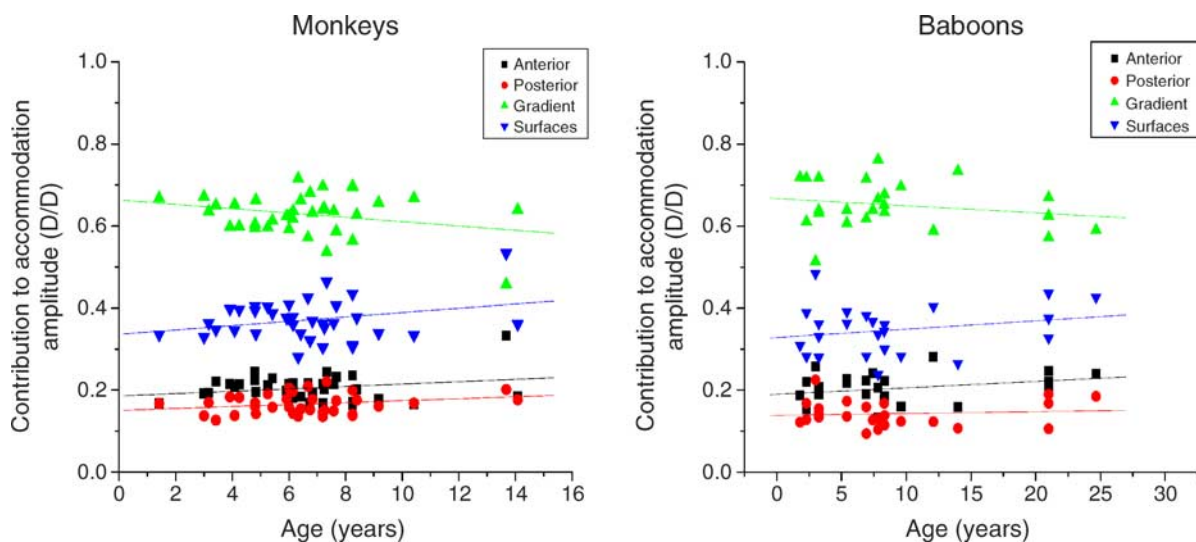

Figure 6. The contributions calculated for the lens anterior surface, posterior surface, combined surfaces, and gradient with respect to accommodation amplitude plotted as a function of age for (left) cynomolgus monkeys and (right) hamadryas baboons.
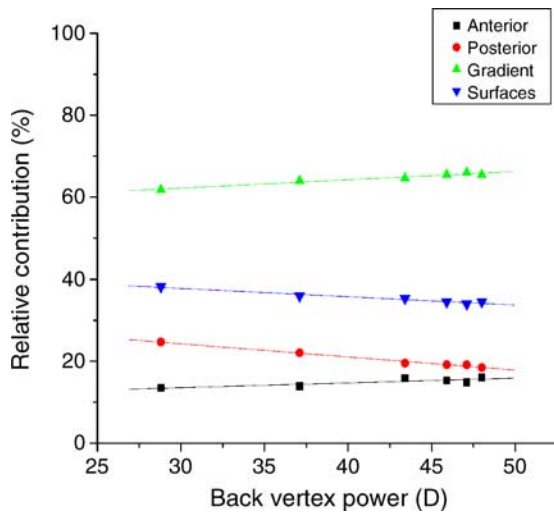
Figure 7. Example of the relative contribution (%) of the lens anterior surface, posterior surface, combined surfaces, and gradient to back vertex power of the lens during simulated accommodation (baboon, age = 6.92 years). In this lens, there is a statistically significant change in the relative contribution of the gradient during accommodation, from 62% to 66%. The relative contribution of the anterior surface decreases and the relative contribution of the posterior surface increases with accommodation. In the majority of lenses (28 monkey lenses and 21 baboon lenses), the relative contribution of the gradient remained constant.

the contributions of the surfaces or gradient to accommodation amplitude (Figure 6).

Relative contributions of the surfaces and gradient to lens power

During stretching (disaccommodation), the relative contribution (in % of the lens back vertex power) of the anterior lens surface decreases and the relative contribution of the posterior lens surface increases (Figure 7). The decrease in relative contribution of the anterior surface of the lens is consistent with the fact that the anterior surface of the lens flattens more than the posterior surface during disaccommodation (Dubbelman & Van der Heijde, 2001; Dubbelman, Van der Heijde, & Weeber, 2005; Koretz, Cook, & Kaufman, 1997). A regression analysis showed that the contribution of the gradient was constant in 28 monkey lenses and 21 baboon lenses ($p > 0.05$). There was a significant change in the relative contribution of the gradient in 8 monkey lenses and 4 baboon lenses; however, this change was always less than 6%.

Since the relative contributions of the gradient and combined surfaces to the lens power are independent of the accommodative state, we can use the unstretched (accommodated) state to illustrate the changes with age for all the primates in this study. The relative contribution of the gradient remains constant with age in both species (Figure 8). The contributions of the anterior surface, posterior surface, and gradient to the lens back vertex power ranged from 13 to 20%, 17 to 23%, and 56 to 70% for the cynomolgus monkeys and from 10 to 17%, 13 to 24%, and 60 to 75% for the hamadryas baboons. The relative contributions are similar in cynomolgus monkeys and hamadryas baboons.

baboons), with a range from 0.44 D/D to 0.68 D/D for cynomolgus monkeys and from 0.51 D/D to 0.76 D/D for hamadryas baboons. There is no major difference between cynomolgus monkeys and hamadryas baboons in
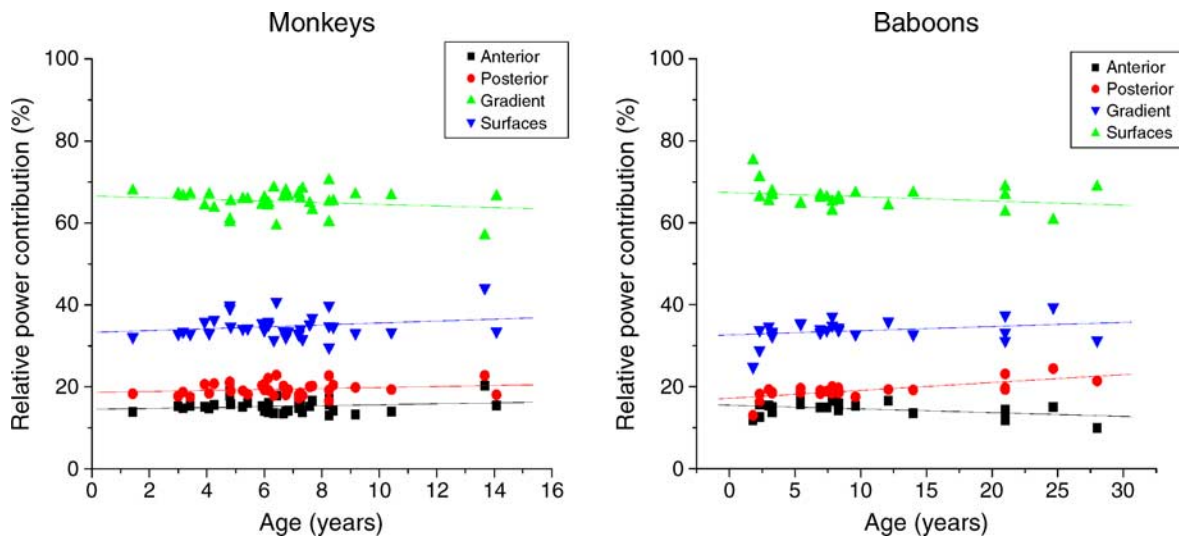

Figure 8. The relative contributions of the anterior surface, posterior surface, combined surfaces, and gradient to the lens back vertex power in the unstretched (accommodated state) plotted as a function of age for (left) cynomolgus monkeys and (right) hamadryas baboons. The relative contribution of the gradient remains constant (monkeys: $p = 0.28$, average = 65 ± 3%; baboons: $p = 0.19$, average = 66 ± 3%).

Discussion

The aim of this study was to determine the contribution of the lens gradient refractive index to the change in lens back vertex power during simulated accommodation in primate lenses. The main findings of the study are:

1. The power, in D, of the lens surfaces and gradient linearly increases with increasing lens power during accommodation.
2. The contribution, in D/D, of the anterior lens surface to the accommodation amplitude is greater than the contribution of the posterior surface for all lenses.
3. The gradient contributes significantly to the accommodation amplitude, corresponding on average to 65% for cynomolgus monkeys and 66% for hamadryas baboons.
4. The lens back vertex power and the power of the surfaces and gradient decrease with age.
5. The relative contribution of the gradient to the accommodative amplitude remains constant with age.

Clearly, the calculated gradient contribution depends on the value of the outer cortex refractive index. We used an outer cortex refractive index of 1.365, derived from measurements of protein concentrations (Moffat et al., 2002; Pierscionek, Smith, & Augusteyn, 1987). This value is also the median of published data, which ranges from 1.34 to 1.39 (Jones et al., 2005; Moffat et al., 2002; Nakao, Ono, Nagata, & Iwata, 1969; Pierscionek & Chan, 1989; Pomerantzeff, Pankratov, Wang, & Dufault, 1984). In any case, independent of the refractive index value selected within this range, we find that our main conclusion that the gradient contributes to the accommodative power of the lens remains valid. In the extreme cases, $n = 1.34$ results in a gradient power contribution of 94% and $n = 1.39$ results in a gradient power contribution of 21%.

Our results are comparable to the *in vivo* human results of Dubbelman et al. (2005), which measured the changes in lens shape in response to an accommodative stimulus. Dubbelman et al. (2005) found a curvature change of 6.7 mm^{-1}/D for the anterior surface and 3.7 mm^{-1}/D for the posterior surface, which corresponds to power changes of 0.19 D/D for the anterior surface and 0.11 D/D for the posterior surface assuming a surface refractive index of 1.365. The combined contribution of the surfaces is therefore 30%, which is comparable to our findings (∼34%). Furthermore, we compared our results with those obtained *in vivo* with Rhesus monkeys by Rosales, Wendt, Marcos, and Glasser (2008). For this comparison, we performed a linear fit on their average anterior and posterior lens curvatures ($R_a = 11.11$ mm $- 6.4$ mm/D; $R_p = -6.64$ mm $+ 0.17$ mm/D) and used the methods from our study to calculate the surface contributions. The resulting contributions were 18.2% for the anterior surface

and 14.5% for the posterior surface, which gives a combined surface contribution of 32.7%. This is also in good agreement with our data and the human results of Dubbelman. In addition, our finding that the gradient power (D) decreases with age is in agreement with *in vitro* and *in vivo* studies on human, cynomolgus, rhesus, and baboon lenses (Borja et al., 2008; Borja, Manns et al., 2010; Dubbelman & Van der Heijde, 2001; Jones et al., 2005). These studies show that this decrease in the gradient power is the main contribution to the loss of power in isolated lenses with age.

To further compare our results with previous studies, which quantified the power of the internal structure of the lens using an equivalent refractive index, we first need to determine the relation between the power of the gradient and the equivalent refractive index. To simplify the analysis, we used a thin lens model. With some arithmetic manipulation, one can show that the relation between equivalent refractive index and power of the gradient is

$$n_{eq} = n_o + (n - n_o)\frac{1}{1 - \frac{P_g}{P}}, \qquad (3)$$

where $n_o = 1.336$ is the refractive index of the aqueous, $n = 1.365$ is the refractive index of lens outer cortex, P is the lens power, and P_g is the contribution of the gradient. Equation 3 shows that equivalent refractive index is a measure of the relative contribution of the gradient to the total lens power (ratio P_g/P). Our finding that the relative contribution of the gradient remains constant with accommodation is therefore in agreement with previous studies, which found that the equivalent refractive index of the lens does not change with accommodation (Garner & Smith, 1997; Hermans et al., 2008).

The finding that the gradient contributes significantly to the accommodation amplitude is consistent with Gullstrand's intracapsular theory of accommodation and the previous observation by Garner and Smith (1997) based on a gradient model of the lens. Gullstrand used a higher value for the equivalent refractive index for his schematic lens in the accommodated state to take into account the contribution of the gradient. Our results, together with the simplified model of Equation 3, show that a constant value for the equivalent index with accommodation can be assumed since the relative contribution of the gradient remains constant.

Our observation that the relative contribution of the gradient remains constant with age is consistent with the results of a previous study on isolated cynomolgus and rhesus monkey lenses (Borja, Manns et al., 2010), where the gradient contribution was found to be 62% on average for cynomolgus monkeys. The values in the present study are slightly higher (65%) mainly because of differences in the value for the cortex refractive index (1.371 versus 1.365) and different methodology to calculate the lens power (effective power versus back vertex power). On the

other hand, the previous study found a decrease in the relative contribution of the gradient with age in baboon lenses. However, the study only had two older baboon lenses (above 20 years) and had a smaller sample size. With the additional data and broader age range, the present study shows that the relative gradient contribution is constant with age.

Age-related changes in gradient power (D) seem to be primarily due to changes in the axial refractive index profile of the lens (Augusteyn, 2010; Augusteyn et al., 2008; Jones et al., 2005). On the other hand, the fact that the relative contribution of the gradient remains constant with accommodation suggests that the changes in gradient power with accommodation are not due to changes in the axial distribution but rather to changes of the iso-indicial curvatures with accommodation. This observation is consistent with *in vivo* MRI studies showing that the axial gradient profile changes much less with accommodation than with age (Kasthurirangan et al., 2008).

In all lenses, we observed only a small change in posterior lens curvature during accommodation, consistent with previous *in vivo* studies on human and rhesus monkey lenses (Brown, 1974; Dubbelman et al., 2005; Koretz, Bertasso, Neider, True-Gabel, & Kaufman, 1987; Koretz, Handelman, & Brown, 1984). However, there is always some uncertainty in the measurement of the posterior lens curvature because the posterior lens is imaged through the anterior surface and gradient (Borja et al., 2008, Dubbelman & Van der Heijde, 2001). In the present study, there are two potential sources of error. First, the OCT images were scaled by dividing the optical path length by an estimate of the group refractive index based on previous measurements (Uhlhorn et al., 2008). Second, the OCT images were corrected for distortions due to refraction assuming a uniform refractive index equal to the average index of the lens. We performed an analysis to determine how the value of the group refractive index used to scale the lens and correct posterior distortions affects the posterior lens power. For average group refractive indices ranging from 1.39 to 1.42 (Uhlhorn et al., 2008), we found a variation of less than 0.5 D (5%) for the posterior surface power. Therefore, the uncertainty on the value of the average refractive index has only a minimal effect on the final results.

In conclusion, we find that the gradient contributes on average $65 \pm 3\%$ of the total lens power change during accommodation for cynomolgus monkeys and $66 \pm 3\%$ for hamadryas baboons, assuming an outer cortex refractive index of 1.365. The relative contribution of the gradient (or equivalent refractive index) remains constant with accommodation. These findings show that accommodation-dependent optical models of the lens can assume a constant equivalent refractive index. They also suggest that a material of uniform refractive index could serve as a lens substitute for lens refilling procedures to restore accommodation (Kessler, 1964; Koopmans, Terwee, Barkhof, Haitjema, & Kooijman, 2003; Nishi, Mireskandari, Khaw, & Findl, 2009; Parel, Gelender, Trefers, & Norton, 1986). Overall, our findings lend support to the intracapsular theory of accommodation of Gullstrand.

Disclosure: B. M. Maceo, none; F. Manns, none; D. Borja, none; D. Nankivil, none; S. Uhlhorn, none; E. Arrieta, none; A. Ho, none; R. C. Augusteyn, none; J.-M. Parel, none.
Commercial relationships: none.
Corresponding author: Fabrice Manns.
Email: fmanns@miami.edu.
Address: Bascom Palmer Eye Institute, 1638 NW 10 Avenue, Miami, FL 33136, USA.

References

Atchison, D. A., & Smith, G. (2000). *Optics of the human eye*. Oxford, UK: Butterworth-Heinemann.

Atchison, D. A., & Smith, G. (2005). Chromatic dispersions of the ocular media of human eyes. *Journal of the Optical Society of America, 22,* 29–37.

Augusteyn, R. C. (2010). On the growth and internal structure of the human lens. *Experimental Eye Research, 90,* 643–654.

Augusteyn, R. C., Jones, C. E., & Pope, J. M. (2008). Age-related development of a refractive index plateau in the human lens: Evidence for a distinct nucleus. *Clinical and Experimental Optometry, 91,* 296–301.

Borja, D., Manns, F., Ho, A., Ziebarth, N., Rosen, A. M., Jain, R., et al. (2008). Optical power of the isolated human crystalline lens. *Investigative Ophthalmology & Visual Science, 49,* 2541–2548.

Borja, D., Manns, F., Ho, A., Ziebarth, Z. M., Acosta, A. C., Arrieta-Quintera, E., et al. (2010). Refractive power

and biometric properties of the nonhuman primate isolated crystalline lens. *Investigative Ophthalmology & Visual Science, 51,* 2118–2125.

Borja, D., Siedlecki, D., de Castro, A., Uhlhorn, S., Ortiz, S., Arrieta, E., et al. (2010). Distortions of the posterior surface in optical coherence tomography images of the isolated crystalline lens: Effect of the lens index gradient. *Biomedical Optics Express, 1,* 1331–1340.

Brown, N. P. (1974). The change in lens curvature with age. *Experimental Eye Research, 19,* 175–183.

de Castro, A., Siedlecki, D., Borja, D., Uhlhorn, S., Parel, J.-M., Manns, F., & Marcos, S. (2011). Age-dependent variation of the gradient index profile in human crystalline lenses. *Journal of Modern Optics,* doi:10.1080/09500340.2011.565888. [Article]

Dubbelman, M., & Van der Heijde, G. L. (2001). The shape of the aging human lens: Curvature, equivalent refractive index and the lens paradox. *Vision Research, 41,* 1867–1877.

Dubbelman, M., Van der Heijde, G. L., & Weeber, H. A. (2005) Change in shape of the aging human crystalline lens with accommodation. *Vision Research, 45,* 117–132.

Ehrmann, K., Ho, A., & Parel, J.-M. (2008). Biomechanical analysis of the accommodative apparatus in primates. *Clinical and Experimental Optometry, 91,* 302–312.

Garner, L. F., & Smith, G. (1997). Changes in equivalent and gradient refractive index of the crystalline lens with accommodation. *Ophthalmology & Visual Science, 74,* 114–119.

Glasser, A., & Campbell, M. C. (1999). Biometric, optical and physical changes in the isolated human crystalline lens with age in relation to presbyopia. *Vision Research, 39,* 1991–2015.

Gullstrand, A. (1909). Mechanism of accommodation. In H. H. Helmholtz von (Ed.), *Handbuch der physiologischen optik* (Appendix IV, pp. 383–415). (*Helmholtz's treatise in physiological optics,* J. P. C. Southall, Trans.). New York: Dover. (Original work published 1962).

Gullstrand, A. (1911). *How I found the mechanism of intracapsular accommodation. Nobel Lecture December 11, 1911. Nobel Lectures, Physiology or Medicine 1901–1921.* Amsterdam, The Netherlands: Elsevier Publishing Company.

Hermans, E. A., Dubbelman, M., Van der Heijde, R., & Heethaar, R. M. (2008). Equivalent refractive index of the human lens upon accommodative response. *Optometry and Vision Science, 5,* 1179–1184.

Jenkins, F. A., & White, H. E. (1976). *Fundamentals of optics.* New York: McGraw-Hill.

Jones, C. E., Atchison, D. A., Meder, R., & Pope J. M. (2005). Refractive index distribution and optical properties of the isolated human lens measured using magnetic resonance imaging (MRI). *Vision Research, 45,* 2352–2366.

Kasthurirangan, S., Markwell, E. L., Atchison, D. A., & Pope, J. M. (2008). In vivo study of changes in refractive index distribution in the human crystalline lens with age and accommodation. *Investigative Ophthalmology & Visual Science, 49,* 2531–2540.

Kessler, J. (1964). Experiments in refilling the lens. *Archives of Ophthalmology, 71,* 412–417.

Koopmans, S. A., Terwee, T., Barkhof, J., Haitjema, H. J., & Kooijman, A. J. (2003). Polymer refilling of presbyopic human lenses in vitro restores the ability to undergo accommodative changes. *Investigative Ophthalmology & Visual Science, 44,* 250–257.

Koretz, F. K., Bertasso, A. M., Neider, M. W., True-Gabelt, B., & Kaufman P. L. (1987). Slit-lamp studies of the rhesus monkey eye: II. Changes in crystalline lens shape, thickness and position during accommodation and aging. *Experimental Eye Research, 45,* 317–326.

Koretz, F. K., Cook, C. A., & Kaufman, P. L. (1997). Accommodation and presbyopia in the human eye. Changes in the anterior segment and crystalline lens with focus. *Investigative Ophthalmology & Visual Science, 38,* 569–578.

Koretz, F. K., Handelman, G. H., & Brown, N. P. (1984). Analysis of human crystalline lens curvature as a function of accommodative state and age. *Vision Research, 24,* 1141–1151.

Manns, F., Parel, J.-M., Denham, D., Billotte, C., Ziebarth, N., Borja, D., et al. (2007). Optomechanical response of human and monkey lenses in a lens stretcher. *Investigative Ophthalmology & Visual Science, 48,* 3260–3268.

Moffat, B. A., Atchison, D. A., & Pope, J. M. (2002). Age-related changes in refractive index distribution and power of the human lens as measured by magnetic resonance micro-imaging in vitro. *Vision Research, 42,* 1683–1693.

Nakao, S., Ono, T., Nagata, R., & Iwata, K. (1969). Model of refractive indices in the human crystalline lens. *Japanese Journal of Clinical Ophthalmology, 23,* 903–906.

Nankivil, D., Manns, F., Arrieta-Quintero, E., Ziebarth, N., Borja, D., Amelinckx, A., et al. (2009). Effect of anterior zonule transection on the change in lens diameter and power in cynomolgus monkeys during simulated accommodation. *Investigative Ophthalmology & Visual Science, 50,* 4017–4021.

Nishi, Y., Mireskandari, K., Khaw, P., & Findl, O. (2009). Lens refilling to restore accommodation. *Journal of Cataract & Refractive Surgery, 35,* 374–382.

Parel, J.-M., Gelender, H., Trefers, W. F., & Norton, E. W. D. (1986). Phaco-Ersatz: Cataract surgery designed to preserve accommodation. *Graefe's Archive for Clinical and Experimental Ophthalmology, 224,* 165–173.

Pierscionek, B., Smith, G., & Augusteyn, R. C. (1987). The refractive increments of bovine α-, β- and γ-crystallins. *Vision Research, 27,* 1539–1541.

Pierscionek, B. K., & Chan, D. Y. (1989). Refractive index gradient of human lenses. *Optometry and Vision Science, 66,* 822–829.

Pomerantzeff, O., Pankratov, M., Wang, G. J., & Dufault, P. (1984). Wide-angle optical model of the eye. *Journal of Optometry and Physiological Optics, 61,* 166–176.

Rosales, P., Wendt, M., Marcos, S., & Glasser A. (2008). Changes in crystalline lens radii of curvature and lens tilt and decentration during dynamic accommodation in rhesus monkeys. *Journal of Vision, 8*(1):18, 1–12, http://www.journalofvision.org/content/8/1/18, doi:10.1167/8.1.18. [PubMed] [Article]

Smith, G. (2003). The optical properties of the crystalline lens and their significance. *Clinical and Experimental Optometry, 81,* 3–18.

Tabernero, J., Berrio, E., & Artal, P. (2011). Modeling the mechanism of compensation of aberrations in the human eye for accommodation and aging. *Journal of the Optical Society of America A, 28,* 1889–1895.

Uhlhorn, S. R., Borja, D., Manns, F., & Parel, J.-M. (2008). Refractive index measurement of the isolated crystalline lens using optical coherence tomography. *Vision Research, 48,* 2732–2738.

Urs, R., Ho, A., Manns, F., & Parel, J.-M. (2010). Age-dependent Fourier model of the shape of the isolated ex vivo human crystalline lens. *Vision Research, 50,* 1041–1047.